33rd Annual International Conference of the IEEE EMBS
Boston, Massachusetts USA, August 30 - September 3, 2011

Imaging of Sebaceous Glands of Human Skin by Three-dimensional Ultrasound Microscopy and Its Relation to Elasticity

Kazutoshi Kumagai, Hideyuki Koike, Yukina Kudo, Ryo Nagaoka, Kiyono Kubo, Kazuto Kobayashi, Yoshifumi Saijo, *Member, IEEE*

***Abstract*— High frequency ultrasound imaging has realized high resolution in vivo imaging of the biological tissues at a microscopic level. Human skin structure, especially sebaceous glands at the deep part of the dermis, was observed by three-dimensional ultrasound microscopy with the central frequency of 120 MHz. The visco-elasticity and surface sebum level of the observed region were measured by established testing devices. Both sebaceous glands density and surface sebum level were higher in cheek than those in forearm. The viscosity of forearm was lower than that of cheek. These results suggest that sebaceous glands may act as cushions of the skin besides their classical role of secreting sebum and some hormones. High frequency ultrasound imaging contributes to the evaluation of human skin aging.**

I. Introduction

HIGH resolution ultrasound imaging is available by high frequency ultrasound because both wavelength and beam width are inversely proportional to the ultrasonic frequency [1-7]. Routine echography in health care or gynecology uses several MHz ultrasound and its resolution is around 0.5mm. 15 micron resolution is acquired by 100MHz and 1GHz ultrasound realizes 1.5 micron resolution which enables cellular imaging. For example, the microstructure of human skin such as sebaceous glands, hair follicles and capillary blood vessels can be observed with specially developed 3D ultrasound microscopy with the frequency around 100 MHz.

In the aging societies, many people are interested in aging of skin. The elasticity of human skin and sebum level of skin surface can be measured by some established biomechanical testing methods [8, 9].

In the present study, *in vivo* human skin morphology was evaluated by 3D ultrasound microscopy with the ultrasonic frequency of 120 MHz and its relationships were compared to the biomechanical properties measured by biomechanical methods.

Manuscript received June 18, 2011. This project was supported in part by Grants-in-Aid for Scientific Research (Scientific Research (B) 22300175) from the Japan Society for the Promotion of Science, Sendai Advanced Preventive Health Care Services Cluster from the Ministry of Education, Culture, Sports, Science and Technology and Regional Innovation Program from the Ministry of Economy, Trade and Industry.

Kazutoshi Kumagai (e-mail: kazutoshi.kumagai@bme.tohoku.ac.jp), Hideyuki Koike (e-mail: hideyuki.koike@bme.tohoku.ac.jp), Yukina Kudo (e-mail: yukina.kudo@bme.tohoku.ac.jp), Ryo Nagaoka (ryo@ecei.tohoku.ac.jp), Kiyono Kubo (kiyono_k@ecei.tohoku.ac.jp) and Yoshifumi Saijo (Corresponding author, phone: +81-22-717-8514; fax: +81-22-795-5882; e-mail: saijo@idac.tohoku.ac.jp) are with the Graduate School of Biomedical Engineering, Tohoku University, Sendai 980-8579 Japan

Kazuto Kobayashi is with the Honda Electronics Co. Ltd., Toyohashi 441-3193 Japan (e-mail: kazuto@honda-el.co.jp).

II. Methods

A. Instrumental Setup

An electric impulse was generated by a high speed switching semiconductor. The start of the pulse was within 400 ps, the pulse width was 2 ns, and the pulse voltage was 40 V. The frequency of the impulse covered up to 500 MHz. The electric pulse was used to excite a vinylidene fluoride and trifluoroethylene P(VDF-TrFE) transducer. The aperture diameter of the transducer was 2.4 mm, and the focal length was 3.2 mm. The central frequency was 120 MHz, the bandwidth (-6 dB) was 70-170 MHz, and the pulse repetition rate was 10 kHz. The reflections from the tissue was received by the transducer and were introduced into a Windows-based personal computer (PC) (Pentium D, 3.0 GHz, 2GB RAM, 250GB HDD) with a high-speed digitizer card (Acqiris DP210, Geneva, Switzerland). The frequency range was 500 MHz, and the maximum sampling rate was 2 GS/s. Eight pulse echo sequences with 2000 sampling points were averaged for each scan line in order to increase the signal-to-noise-ratio. The transducer was mounted on the X-Y scanner with two linear servo motors that were controlled by XY-scan controller connected to the serial port of the PC.

Fig. 1 shows a block diagram of the 3D ultrasound microscope system.

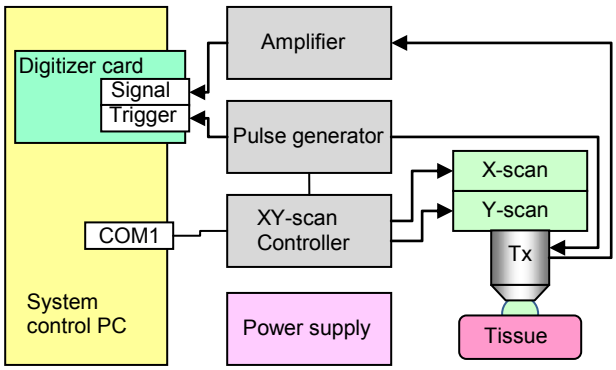

Fig. 1. Block diagram of 3D ultrasound microscope system

B. Image Processing

Obtained RF signal of each scanning line was converted to B-mode image by a conventional image processing algorithm

of echography. The scan area was 4.8 mm wide (X-axis) and 1.5 mm deep (Z-axis) with 300 x 300 pixels. Consecutive 150 B-mode images were reconstructed to volume data. Multi-planar reconstructed (MPR) images parallel to the skin surface were processed. The MPR image at 800-μm beneath the skin surface was observed because sebaceous glands mostly distributed in this layer. As the *ex-vivo* pilot study showed that the low intensity area corresponded to sebaceous gland, the sebaceous glands shown as low intensity regions in the MPR images were marked manually and the areas were measured by using image analysis software (Image J, NIH).

C. Sebum Level of the Skin Surface

Sebumeter® (SM815, Courage and Khazaka, Köln, Germany) can measure sebum level of skin surface directly. The principle of the equipment was the optical penetration [8]. The measurement was not influenced by humidity.

A probe attached with the oil blotting paper was put on the skin surface for 30 s. The degree of transparency of paper was calculated at light receiving section.

D. Skin Visco-elasticity Measurement

Human skin is consisted of three layers such as epidermis, dermis and subcutis. Cutometer® (MPA580, Courage and Khazaka, Köln, Germany) was equipped for evaluating the visco-elasticity of whole layers of skin. This instrument measures the mechanical properties of skin based on the principle of suction elongation, utilizing an optical measuring unit [9].

The probe was put gently on the surface of the ROI. The skin was vacuumed into the circular aperture (φ = 2 mm) by negative pressure from inside the probe. Fig. 2 shows the principle of skin elasticity measurement. The skin returned to normal after the negative pressure was released. The height of the skin was measured throughout the deformation process by a prism with a precision of 0.01 mm. The average of four measurements was used to minimize the error.

$\boldsymbol{U_f}$ was defined as the final distension at the end of the vacuum period and $\boldsymbol{U_r}$ as the immediate relaxation within the first 0.1 s after the end of the vacuum period. The ratio of elastic recovery to the total deformation ($\boldsymbol{U_r}$ / $\boldsymbol{U_f}$) was used as the best parameter.

E. Observation of Human Skin

A seal with square open window was put on each objective area in cheek and forearm to determine the region of interest (ROI) in optical and ultrasound imaging. The CCD camera (2 way microscope INT-100, Integral Corporation, Japan) was used to record the skin surface morphology. Ultraviolet (UV) image of the skin surface was also captured for detecting hair follicles because horny plugs stood out by flashing porphyrin which was produced by *Propionibacterium acnes*.

F. Subjects

Twenty one healthy male subjects with written informed consent (23.4±0.6 y.o.) were evaluated by 3D ultrasound microscope. They didn't have significant skin diseases. The research was approved by an ethical committee of Tohoku University.

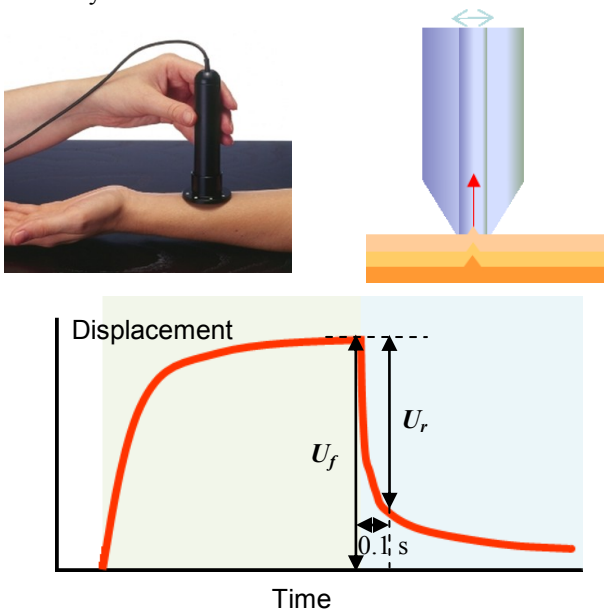

Fig. 2. Principle of skin elasticity measurement

III. Results

A. High Frequency Ultrasound Imaging

Fig. 3 shows the B-mode images of 21-year old male's cheek. The imaged areas are 4.8 x 1.5 mm.

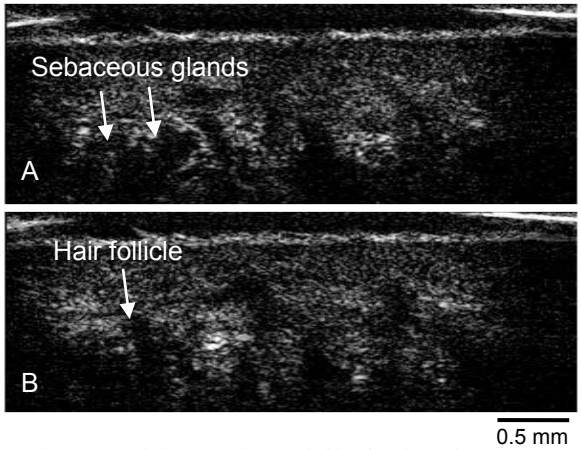

Fig. 3. B-mode images of normal skin showing sebaceous glands and hair follicle

The *in vivo* human skin was able to be observed up to 1.2 mm depth. The three layers, epidermis, dermis and subcutis were able to be observed. In the dermis layer, microstructures such as sebaceous glands, capillary blood vessels and hair follicles can be seen as low echo density area. Fig. 4A is the MPR image beneath 800 μm that is approximately parallel to the skin surface. Fig. 4B and 4C show the skin surface images obtained by CCD camera with normal light and ultraviolet light corresponding to the ultrasound images. The distribution

of the sebaceous glands was more clearly observed on MPR images compared to conventional B-mode images.

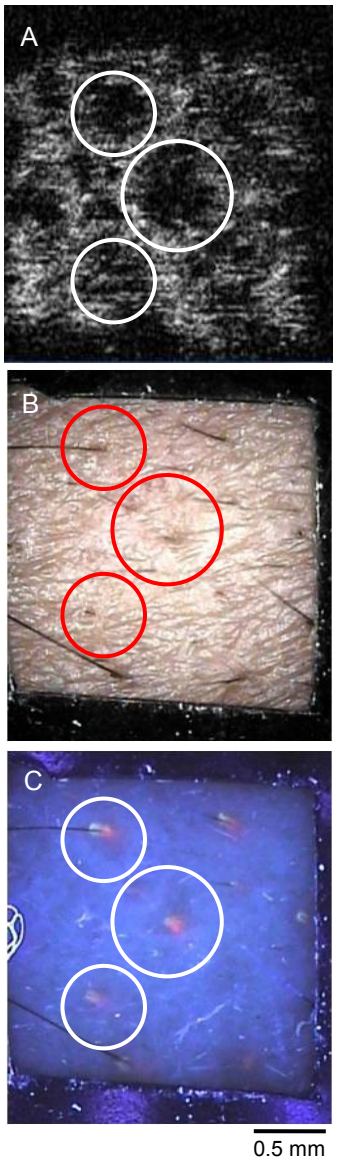

Fig. 4. Ultrasound and optical images of the skin.
A: MPR image beneath 800 μm that is approximately parallel to the skin surface, B: CCD image of the skin surface, C: UV image of the skin surface.

Each circle of the Fig. 4A, 4B and 4C correspond sebaceous glands in MPR image, hair follicle in CCD image and homy plugs in UV image, respectively.

Fig. 5A and 5B show the B-mode images of 24-year old male's forearm. The imaged areas are 4.8 x 1.5 mm. Fig. 5C shows the MPR image beneath 800 μm that is approximately parallel to the skin surface. The morphology in the dermis layer of forearm was more homogeneous than that of the cheek.

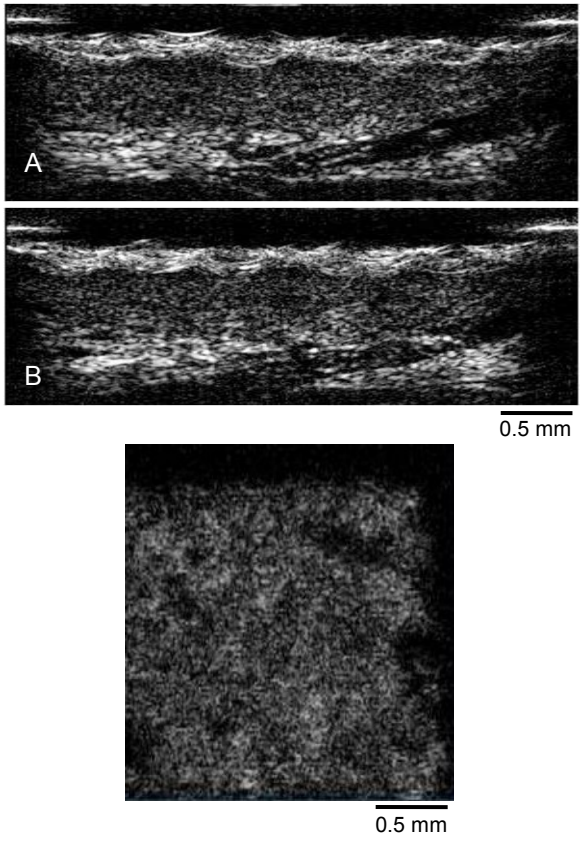

Fig. 5. B-mode and MPR images of normal skin in forearm.
A, B: B-mode images, C: MPR image beneath 800 μm that is approximately parallel to the skin surface.

Fig. 6 is the graph showing density of sebaceous gland in cheek and forearm. Paired t-test is used to compare the values. The density is significantly higher in cheek than that in forearm ($p<0.01$).

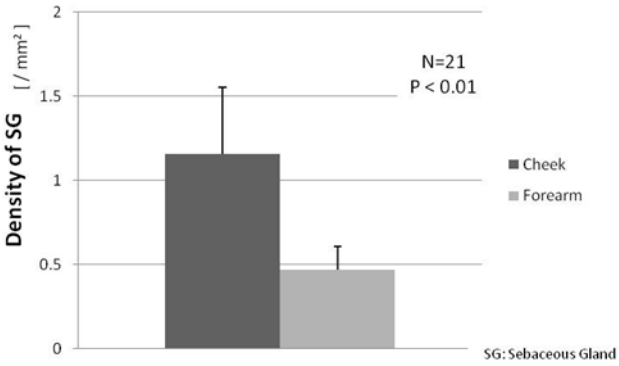

Fig. 6. Density of sebaceous gland (SG) in cheek and forearm.

B. Sebum Level of the Skin Surface

Fig. 7 shows the sebum level of cheek and forearm. Sebum level is significantly higher in cheek ($p<0.01$).

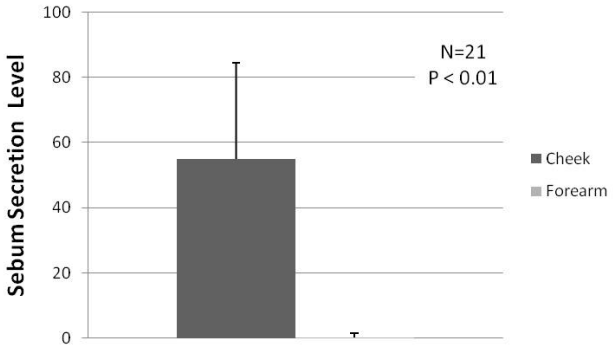

Fig. 7. Surface sebum level of cheek and forearm.

C. Skin Visco-elasticity

Fig. 8 shows the U_r / U_f of cheek and forearm. As the value is inversely proportional to skin viscosity, viscosity of the cheek is significantly higher than that of forearm ($p<0.01$).

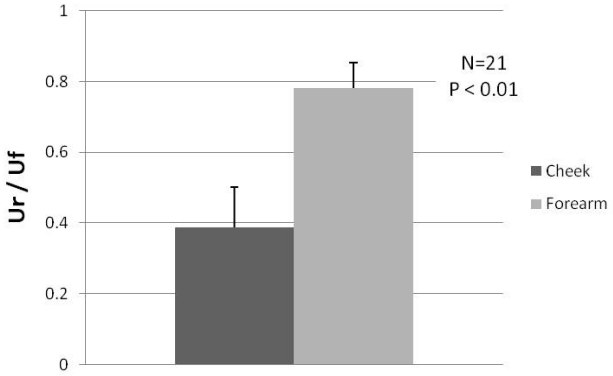

Fig. 8. Skin visco-elasticity of cheek and forearm.

IV. Discussion

A specially developed 3D ultrasound microscope was successful to provide the morphology of human skin more clearly than conventional ultrasonoglaphy. The spatial resolution of the 3D microscope was 20 μm and this was enough for the observation of microstructures such as hair follicles, sebaceous glands and capillary blood vessels. Optical coherence tomography (OCT) provides higher resolution images than ultrasound [10]. However, the penetration depth of the light is limited to approximately 1 mm in human skin and it was not enough to observe whole area where sebaceous glands exist.

Both sebaceous glands density and surface sebum level were higher in cheek than those in forearm. The viscosity of cheek was higher than that of forearm. These results suggest that sebaceous glands may act as cushions of the skin besides their classical role of secreting sebum and some hormones.

The results also contribute to the evaluation of human skin aging. It had been said that the size of sebaceous glands increased with age [11]. The measurement of the sebaceous gland volume may become one of good parameters for assessment of aging of the skin.

V. Conclusions

Human skin structure, especially sebaceous glands at the deep part of the dermis, was observed by three-dimensional ultrasound microscopy with the central frequency of 120 MHz. The elasticity and surface sebum level of the observed region were measured by established biomechanical testing devices. Both sebaceous glands density and surface sebum level were higher in cheek than those in forearm. The viscosity of cheek was higher than that of forearm. These results suggest that sebaceous glands may act as cushions of the skin besides their classical role of secreting sebum and some hormones. High frequency ultrasound imaging contributes to the evaluation of human skin aging.

References

[1] Y. Saijo, M. Tanaka, H. Okawai, H. Sasaki, S. Nitta, F. Dunn, Ultrasonic tissue characterization of infarcted myocardium by scanning acoustic microscopy, *Ultrasound Med Biol* 23 (1997), pp. 77-85.

[2] Y. Saijo, H. Sasaki, H. Okawai, S. Nitta, M. Tanaka, Acoustic properties of atherosclerosis of human aorta obtained with high-frequency ultrasound, *Ultrasound Med Biol* 24 (1998), pp. 1061-1064.

[3] S. El Gammal, C. El Gammal, K. Kaspar, C. Pieck, P. Altmeyer, M. Vogt, H. Ermert, Sonography of the skin at 100 MHz enables in vivo visualization of stratum corneum and viable epidermis in palmar skin and psoriatic plaques, *J Invest Dermatol* 113 (1999), pp.821-9.

[4] Y. Saijo, H. Sasaki, M. Sato, S. Nitta, M. Tanaka, Visualization of human umbilical vein endothelial cells by acoustic microscopy, *Ultrasonics* 38 (2000), pp. 396-399.

[5] Y. Saijo, T. Ohashi, H. Sasaki, M. Sato, C.S. Jorgensen, S. Nitta, Application of scanning acoustic microscopy for assessing stress distribution in atherosclerotic plaque, *Ann Biomed Eng* 29 (2001), pp. 1048-53.

[6] M. Vogt, H. Ermert, In vivo ultrasound biomicroscopy of skin: spectral system characteristics and inverse filtering optimization, *IEEE Trans Ultrason Ferroelectr Freq Control* 54 (2007), pp. 1551-9.

[7] Y. Saijo, N. Hozumi, K. Kobayashi, N. Okada, E. D. Santos Filho, H. Sasaki, T. Yambe, M. Tanaka, Ultrasonic tissue characterization of atherosclerosis by a speed-of-sound microscanning system, *IEEE Trans Ultrason Ferroelectr Freq Control* 54 (2007), pp. 1571-1577.

[8] P. G. Sator, J. B. Schmidt, H. Hönigsmann, Comparison of epidermal hydration and skin surface lipids in healthy individuals and in patients with atopic dermatitis, *J Am Dermatol* 48 (2003), pp. 352-8.

[9] P. Elsner, D. Wilhelm, H. I. Maibach, Mechanical properties of human forearm and vulvar skin, *Br J Dermatol* 22, (1990), pp. 607-614.

[10] T. Gambichlera, G. Moussaa, M. Sanda, D. Sandb, P. Altmeyera, K. Hoffmann, Applications of optical coherence tomography in dermatology, *J Dermatol Sci* 40 (2005), pp. 85-94.

[11] G. Plewig, A. M. Kligman, Proliferative activity of the sebaceous glands of the aged, *J Invest Dermatol* 70 (1978), pp. 314-317.